Uncertainty quantification in covid-19 spread: lockdown effects

Ana Carpio*, Emile Pierret †

September 28, 2021

Abstract. We develop a Bayesian inference framework to quantify uncertainties in epidemiological models. We use SEIJR and SIJR models involving populations of susceptible, exposed, infective, diagnosed, dead and recovered individuals to infer from covid-19 data rate constants, as well as their variations in response to lockdown measures. To account for confinement, we distinguish two susceptible populations at different risk: confined and unconfined. We show that transmission and recovery rates within them vary in response to facts. A key unknown to predict the evolution of the epidemic is the fraction of the population affected by the virus, including asymptomatic subjects. Our study tracks its time evolution with quantified uncertainty from available official data, limited, however, by the data quality. We exemplify the technique with data from Spain, country in which late drastic lockdowns were enforced for months. In late actions and in the absence of other measures, spread is delayed but not stopped unless a large enough fraction of the population is confined until the asymptomatic population is depleted. To some extent, confinement could be replaced by strong distancing through masks in adequate circumstances.

1 Introduction

Since the outbreak of the current covid-19 pandemic [32, 36], Health Services worldwide report daily data about the status of the epidemic, which serve as a guide for the design of non-pharmaceutical interventions [15, 22]. An increasing number of mathematical studies assess the efficacy of different policies [1, 4, 5, 11, 17, 22]. Moreover, mathematical models and data analysis are employed to estimate relevant epidemiological parameters [13, 22, 24, 28, 29, 34] and to try to forecast the evolution [2, 14, 16, 23, 25, 30, 35]. While some of this research is based on direct data analysis [22, 29], machine learning techniques [2, 35] or empirical laws for different populations [17], the use of balance equations to predict population dynamics is a common approach.

After the pioneering work of Kermack and McKendrick [21], SIR type models have become a standard tool in epidemiological studies [12]. The specific structure of the selected models depends on the available information and on assumptions about the epidemic spread [18]. Basic SIR models involve populations of susceptible S, infected I, and recovered R individuals, expecting immunity of the latter [3, 11, 16, 34]. SEIR variants distinguish also the individuals exposed to the virus E,

---

*Departamento de Matemática Aplicada, Universidad Complutense, 28040 Madrid, Spain, ana_carpio@mat.ucm.es

†CMLA, ENS Paris-Saclay, 91190 Gif-sur-Yvette, France

which may become infective [24, 25]. Immunity of the recovered is suppressed in SEIRS systems [23, 30]. During the 2002-04 SARS (Severe Acute Respiratory Syndrome) outbreak, these models were adapted to describe the SARS epidemic in different countries by singling out the diagnosed infective J [10, 13], becoming SEIJR or SIJR models. Diagnosed individuals are isolated. The virus SARS-CoV-2 responsible for the illness covid-19 belongs to the same family as the virus SARS-CoV, responsible for SARS. The epidemics triggered by them share some features, such as the role of asymptomatic individuals in superspread events, see [28] for a quantification of the fraction of asymptomatic population during covid-19 spread following this approach. Here, we will study the effect of confinement measures on covid-19 spread by distinguishing two susceptible SEIJR populations: confined and non confined.

To have a predictive value, we must fit the model parameters to available data. This can be done applying optimization or adjoint-based data assimilation techniques to reduce the difference between recorded data and model predictions for selected parameters [13, 34], for instance. However, data for epidemiological studies are subject to many sources of noise and uncertainty. In the case of the current covid-19 pandemic, different countries, and regions within them, define the diagnosed, recovered and dead individuals they count in their official reports in different ways. The number of dead individuals may refer only to patients who die in hospitals or include also deaths at homes and care homes. Furthermore, the death of covid patients with previous health issues may be officially attributed to other causes. On the other hand, the number of diagnosed individuals may refer only to cases confirmed by a PCR (Polymerase chain reaction) test or include also positive antibody tests, or probable cases with compatible symptoms and clinical history. Moreover, the results of tests may arrive with a variable delay, which results in fluctuations and exclusions. Undated cases may not be counted at all. Tests repeated for the same individuals may be counted as different. Additionally, the number of tests performed varies largely over the weeks due to supply shortages and changes in local testing policies, and the accuracy of the tests employed may fluctuate, yielding false negatives or positives.

Uncertainty in the data propagates to any predictions based on them. Instead of fixing specific guesses for the model coefficients, it is convenient to explore approaches that quantify uncertainty [5, 7, 11, 17, 28]. Unlike most work which does not distinguish undocumented and documented infected individuals, here we follow the SEIJR approach and compare data to model predictions of diagnosed infected J [10, 13, 28], including quarantine measures for them and taking into account the diagnose rate due to testing. We develop a general framework to infer SEIJR model coefficients from data with quantified uncertainty, taking into account confinement measures as they are sequentially enforced or lifted by means of two populations: confined and unconfined. This allows us to analyze variations in the model rates and in the distributions of the different populations a time grows as a result of the measures implemented, including undiagnosed infected individuals and asymptomatic individuals. We focus on the case of Spain, where drastic late global lockdowns were enforced at the same time in the whole country, producing well differentiated periods in the data along a long time period, see Fig. 1. The situation is quite different from the german case, in which mild measures were implemented very early to curb the spread [11], the italian case, where strength spatiotemporal differences between regions occurred [4, 16], and from studies of initial stages [24, 25]. Nevertheless, our methods apply to data for diagnosed, dead and recovered individuals from any other country. The key idea is introducing a susceptible subpopulation at lower risk, which might also be achieved by milder measures such as generalized distancing through masks instead of confinement in a closed system, no individuals enter or exit the system. The analysis of migration and spatial dynamics are relevant topics [14, 4, 28], still out
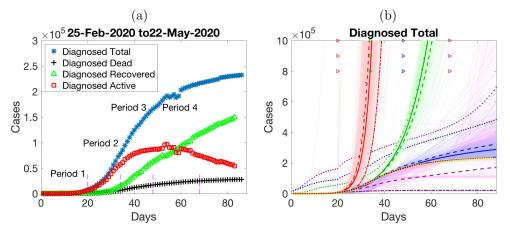
of the scope of the present study.

Figure 1: (a) Daily counts of diagnosed, recovered and dead individuals (PCR confirmed) in Spain since February 25th, 2020, until May 22th, 2020 [6]. After an initial period of uncontrolled spread (Period 1), borders were closed, while all the population being able to work online, or not working in basic activities, was confined at home in the whole country (Period 2): education, administration, tourism, shopping, leisure activities... Lockdown was later extended to all non essential activities (Period 3). Only food and medical supplies, healthcare, security, essential transport and essential production remained active. Confinement was then released by stages, first some workers (Period 4), then the rest, while introducing recommendations for the use of masks and social distancing. (b) SEIJR based Bayesian inference and predictions for the total number of diagnosed individuals using counts from Period 1 (red), Periods 1-2 (green), Periods 1-2-3 (blue) and Periods 1-2-3-4 (magenta). For each of them, top coloured triangles separate the inference from the prediction part of the simulations. True data are marked by yellow circles. Solid curves correspond to best fits, dashed curves and dotted curves to different types of sample averages. Shaded areas and dotted curves define uncertainty regions, see Section 6 for a discussion.

The next sections are organized as follows. Section 2 recalls the structure of SEIJR models. We intend to quantify uncertainty when fitting these models to data from the current covid-19 pandemic. We use the SIJR simplification for the initial stage of the outbreak, before contention measures were taken, and compare to the full SEIJR results. SIJR predictions usually underestimate the total number of affected people. Section 3 explains how to obtain guesses of model parameters, which play the role of prior knowledge for the Bayesian studies in Section 4. Section 5 analyzes the initial stage while Section 6 considers the effect of contention measures, with spanish data. We adapt the SEIJR framework to study parameter uncertainty through the different stages, inferring also key magnitudes such as the time evolution of the number of asymptomatic and undiagnosed individuals affected by the virus, or the global number of affected people. In late interventions, and in the absence of other preventive measures, spread is delayed but not stopped unless a large enough fraction of the population is confined for a long enough time, until the number of asymptomatic and undiagnosed individuals is depleted. Once confinement is over, the usage of masks plays a similar role keeping a fraction of the population at a lower risk in a closed system. Section 7 summarizes our conclusions.

3

2   SEIJR models for SARS and Covid-19 type epidemics

SEIJR models involving populations of susceptible (S), exposed (E), infective (I), diagnosed (J), and recovered (R) individuals were proposed in [10] to study the spread of the 2002-04 SARS outbreak. Here, we will adapt them to describe contention measures for covid-19. Considering two populations S_1 and S_2 of different susceptibility, the model takes the form:

$$
\begin{aligned}
\frac{dS_1}{dt} &= -\beta S_1(t)\frac{I(t) + qE(t) + \ell J(t)}{N}, \\
\frac{dS_2}{dt} &= -\beta p S_2(t)\frac{I(t) + qE(t) + \ell J(t)}{N}, \\
\frac{dE}{dt} &= \beta(S_1(t) + pS_2(t))\frac{I(t) + qE(t) + \ell J(t)}{N} - kE(t), \\
\frac{dI}{dt} &= kE(t) - (\alpha + \gamma_1 + \delta)I(t), \\
\frac{dJ}{dt} &= \alpha I(t) - (\gamma_2 + \delta)J(t), \\
\frac{dR}{dt} &= \gamma_1 I(t) + \gamma_2 J(t), \\
\frac{dD}{dt} &= \delta I(t) + \delta J(t),
\end{aligned}
\tag{1}
$$

where $N = S_1 + S_2 + E + I + J + R + D$ is the total population number, which remains constant. D is the number of dead individuals. The exposed E are a class of asymptomatic and possibly infectious individuals. The possibility of transmission from exposed individuals E is represented by the parameter q. They may progress to the infective state I at a rate k. The class I is composed of symptomatic, infectious, and undiagnosed individuals. Infectious individuals I become diagnosed J at a rate α. The recovery rate of the infective I is γ_1, whereas the recovery rate of the diagnosed J is γ_2. The recovered individuals R keep track of the cumulative number of sick individuals who become healthy again. Diagnosed individuals J are isolated from the rest. Their reduced impact on transmission is represented through a parameter ℓ. Mortality of infected I and diagnosed J individuals caused by the virus is denoted by δ. Finally, β represents the transmission rate: how susceptible S individuals become virus spreaders. Time is measured in days.

The model has to be complemented with initial conditions. This fact introduces an additional parameter t_{in} to locate the time at which local spread started [13]. Other approaches assume the initial data unknown instead [11], in our case that choice would increase considerably the number of unknowns. Furthermore, we consider that the risk of infection for S_2 is lower than the risk for S_1 by a factor p. The total population is partitioned as $S_1 = (1 - \rho)S$, $S_2 = \rho S$, ρ being the fraction of the susceptible population S at a lower risk of infection. The risk might vary due to specific characteristics of the population (age, sex, genes) [10]. Here, variations will be due to confinement/protection measures enforced on part of the population.

Two constraints are usually imposed on the parameters: 1) $\alpha > \gamma_1$ and 2) $\gamma_2^{-1} = \gamma_1^{-1} - \alpha^{-1}$ [10]. Moreover, the following expression for the basic reproduction number [10] holds

$$
\mathcal{R}_0 = \beta(\rho + p(1 - \rho))\left(\frac{q}{k} + \frac{1}{\alpha + \gamma_1 + \delta} + \frac{\alpha\ell}{(\alpha + \gamma_1 + \delta)(\gamma_2 + \delta)}\right).
$$

The reproduction number represents the expected number of cases immediately originated by one

Par.	Definition	Guess
β	Transmission rate per day	
k	Rate of progression to the infectious state per day	
α	Rate of progression from infective to diagnosed per day	1/5-1/6 (stats)
γ_1	Rate at which infectious individuals recover per day	$\gamma_1^{-1} = \gamma_2^{-1} + \alpha^{-1}$
γ_2	Rate at which diagnosed individuals recover per day	1/10-1/11 (stats)
δ	covid-19 induced mortality per day	1/10-1/11 (stats)
ℓ	Relative measure of isolation of diagnosed cases	1/14 (practice)
q	Relative measure of infectiousness for the exposed	
p	Reduction in risk of covid-19 infection for class S_2	
t_{in}	Time at which local spread starts	
ρ	Fraction of the population at a lower risk	

Table 1: SEIJR model parameters. Guesses from clinical observation when available [19].

case in a population where all individuals are susceptible to infection, that is, no other individuals are infected or immunized (naturally or through vaccination). Instead, the effective reproduction number $\mathcal{R}_e$ is just the number of cases produced in the current state of a population.

This type of models reproduces crudely some characteristics observed in SARS epidemics, such as the emergence of symptomatic and asymptomatic individuals, superspread events and unequal susceptibility, for instance. We will use them here with data from the current covid-19 epidemic. First guesses for some of the model parameters can be estimated from average observations, see Table I. First guesses for two key parameters, t_{in} and β can be obtained from simplified SIJR approximations, as we explain in the next section.

3   Fitting the initial stages of the outbreak

The SEIJR models we have introduced assume that 1) spread takes place in a closed system, 2) the death rate is the same for everybody (death by other causes is neglected), 3) the recovered have immunity, 4) the diagnosed are isolated, and 5) time delays in responses are neglected. Assuming further that: 6) the exposed phase E is neglected, 7) the susceptibility degree is not distinguished $S_1 = S_2 = S$, $p = 1$, 8) the infected are a small fraction of the whole population, so that $\frac{S}{N} \sim 1$,

we obtain a SIJR simplification [13]:

$$\frac{dS}{dt} = -\beta(I + \ell J), \tag{2}$$

$$\frac{dI}{dt} = (\beta - (\alpha + \gamma_1 + \delta))I + \ell\beta J, \tag{3}$$

$$\frac{dJ}{dt} = \alpha I - (\gamma_2 + \delta)J, \tag{4}$$

$$\frac{dR}{dt} = \gamma_1 I + \gamma_2 J, \tag{5}$$

$$\frac{dD}{dt} = \delta(I + J), \tag{6}$$

$$N = S + I + J + R + D, \tag{7}$$

$$S(t_{\text{in}}) = N - 1, \ I(t_{\text{in}}) = 1, \ J(t_{\text{in}}) = R(t_{\text{in}}) = 0 = D(t_{\text{in}}). \tag{8}$$

Here, $N = S + I + J + R + D$ is the total population number, which remains constant. SIJR models allow us to fit important parameters, such as the transmission rate β and the onset of local spread t_{in}, which determine the exponential growth in the initial stages. Their solutions admit analytic expressions, detailed in Appendix 8. Thanks to that fact, they have been used to analyze the influence of isolation measures on the inflexion point, see [13] and references therein. Notice that sign balances in (3) govern the increase of the number of infected people.

In the SIJR model (2)-(8), we have to fit the parameters α, γ_1, γ_2, δ, ℓ, β, as well as t_{in}, defined as the time at which $I(t_{\text{in}}) = 1$. This can be done starting from educated guesses and optimizing a cost functional with respect to them. The clinical information collected during the current pandemic [19] yields tentative average values for the rates α, γ_1, γ_2, δ, and for ℓ, collected in Table 1. We then seek to fit the remaining parameters by optimizing a cost. A popular choice is

$$f(\beta, t_{\text{in}}) = \frac{1}{2}\sum_{j=1}^{L}(\tilde{J}(\beta, j + t_{\text{in}}) - \tilde{y}_j)^2, \tag{9}$$

where $\tilde{y}_j$, $j = 1, ..., L$, are cumulative numbers of diagnosed people for L days and the cumulative variable $\tilde{J}$ solves $\tilde{J}' = \alpha I$, $\tilde{J}(0) = 0$, with I given by (3). This variable $\tilde{J}$ is in fact the total cumulative number of diagnosed individuals, obtained adding to J the diagnosed recovered R_J and the diagnosed dead D_J, solutions of

$$R'_J = \gamma_2 J, \quad D'_J = \delta J, \quad R_J(t_{\text{in}}) = D_J(t_{\text{in}}) = 0. \tag{10}$$

This is an important distinction. Note that equation (4) discounts the diagnosed people who recover or die, thus J tracks only the active diagnosed cases. In practice, only the the diagnosed recovered R_J, the diagnosed dead D_J and the diagnosed active J or total $\tilde{J}$ are recorded by Health Care Systems, since the contribution coming from undiagnosed infected cases is unknown.

SIJR models are particularly adequate for these fittings because solutions admit explicit expressions which reduce numerical errors when dealing with exponentially growing solutions, see Appendix 8. We will resort to the Levenberg-Marquardt-Fletcher algorithm [26] to optimize the costs.
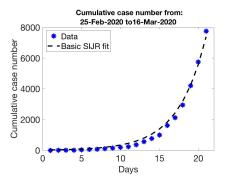
Figure 2: Parameter guess for the first period of data in Fig 1 (free spread): $t_{\mathrm{in}} = 12.3388$, $\beta = 0.6262$, $\alpha = 1/5$, $\gamma_1 = 1/15$, $\gamma_2 = 1/10$, $\delta = 1/10$, $\ell = 1/14$.

The final values we obtain for t_{in} and β are 12 days and 0.6262, starting the optimization from initial guesses 10 and 0.6. This is consistent with the fact that deaths occurred as early as February 13 in Spain were proven to be caused by covid-19. Notice that we are fitting a cumulative magnitude $\tilde{J} = J + R_J + D_J$. Even if the fitting for $\tilde{J}$ is accurate, as Fig 2 shows, the results worsen noticeably when we use these parameters to calculate J, R_J, and D_J and compare with the data recorded for each of them.

We could improve the overall guess using these values as starting point for an algorithm optimizing the cost

$$f(\alpha, \gamma_2, \delta, \ell, \beta, t_{\mathrm{in}}) = \frac{1}{2} \sum_{j=1}^{L} (\tilde{J}(\alpha, \gamma_2, \delta, \ell, \beta, j + t_{\mathrm{in}}) - \tilde{y}_j)^2, \tag{11}$$

with respect to all of the parameters, or resorting to more detailed cost functionals. However, our goal here is to quantify uncertainty in usual rough fits and predictions obtained with them. Therefore, we will use them as priors for the subsequent Bayesian studies.

4   Uncertainty quantification by Bayesian techniques

Bayes' theorem describes the probability of an event, based on prior knowledge about it [20]. According to it, the posterior probability of observing a finite number of parameters $\boldsymbol{\nu}$ given data $\mathbf{d}$ would be

$$p(\boldsymbol{\nu}|\mathbf{d}) = \frac{p(\mathbf{d}|\boldsymbol{\nu})p(\boldsymbol{\nu})}{p(\mathbf{d})}$$

where $p(\mathbf{d}|\boldsymbol{\nu})$ is a conditional probability (the likelihood of observing data $\mathbf{d}$ given parameters $\boldsymbol{\nu}$), and $p(\boldsymbol{\nu})$ represents our prior knowledge on the parameters $\boldsymbol{\nu}$. The normalization factor $p(\mathbf{d})$ represents the probability of the data. It is also a marginal probability, which can be obtained integrating $p(\mathbf{d}|\boldsymbol{\nu})p(\boldsymbol{\nu})$ with respect to $\boldsymbol{\nu}$.

Let us fit our problem in this framework. The parameters are the model parameters, that is,

$$\boldsymbol{\nu} = (t_{\mathrm{in}}, \beta, \gamma_2, \delta, \alpha, \ell), \quad \gamma_1^{-1} = \gamma_2^{-1} + \alpha^{-1}, \tag{12}$$

for the SIJR model or, for SEIJR,

$$\boldsymbol{\nu} = (t_{\text{in}}, \beta, \gamma_2, \delta, \alpha, \ell, q, p, k), \quad \gamma_1^{-1} = \gamma_2^{-1} + \alpha^{-1}. \tag{13}$$

Then, the prior distribution, the likelihood and the posterior distribution are defined as follows.

4.1 Prior distribution

For the prior distribution, we use a parameter guess $\boldsymbol{\nu}_0$ as the mean of a multivaluate normal distribution with a covariance matrix $\mathbf{G}_{\text{pr}}$ constructed from the deviations of each variable

$$p(\boldsymbol{\nu}) = \frac{1}{(2\pi)^{n/2}} \frac{1}{\sqrt{|\mathbf{G}_{\text{pr}}|}} \exp(-\tfrac{1}{2}(\boldsymbol{\nu} - \boldsymbol{\nu}_0)^t \mathbf{G}_{\text{pr}}^{-1}(\boldsymbol{\nu} - \boldsymbol{\nu}_0)), \tag{14}$$

where n is the number of parameters. We choose a diagonal covariance matrix $\mathbf{G}_{\text{pr}}$ with elements σ_i^2, $i = 1, ..., n$. In practice, we have to modify this proposal because our parameters are always positive and gaussians may produce negative values. Thus, we set

$$p_{\text{pr}}(\boldsymbol{\nu}) = \begin{cases} \exp(-\tfrac{1}{2}(\boldsymbol{\nu} - \boldsymbol{\nu}_0)^t \mathbf{G}_{\text{pr}}^{-1}(\boldsymbol{\nu} - \boldsymbol{\nu}_0)), & \nu_j \geq 0, j = 1, ..., n, \\ 0, & \nu_j < 0, \text{ for some } j. \end{cases} \tag{15}$$

This will be our choice of prior distribution $p_{\text{pr}}(\boldsymbol{\nu})$. We do not need to calculate the normalization factor for later use, since our sampling techniques do not require it.

4.2 Likelihood

For the conditional probability density $p(\mathbf{d}|\boldsymbol{\nu})$ we set

$$p(\mathbf{d}|\boldsymbol{\nu}) = \frac{1}{(2\pi)^{L/2}\sqrt{|\mathbf{G}_{\text{n}}|}} \exp\left(-\frac{1}{2}\|\mathbf{f}(\boldsymbol{\nu}) - \mathbf{d}\|_{\mathbf{G}_{\text{n}}^{-1}}^2\right), \tag{16}$$

where $\|\mathbf{v}\|_{\mathbf{G}_{\text{n}}^{-1}}^2 = \bar{\mathbf{v}}^t \mathbf{G}_{\text{n}}^{-1} \mathbf{v}$, $\mathbf{G}_{\text{n}}$ being the covariance matrix representing the noise in the data $\mathbf{d}$, and $\mathbf{f}(\boldsymbol{\nu})$ the observation operator. We assume additive Gaussian noise, i.e., the observations and true parameters would be related by

$$\mathbf{d} = \mathbf{f}(\boldsymbol{\nu}_{true}) + \boldsymbol{\varepsilon}. \tag{17}$$

Here, the noise $\boldsymbol{\varepsilon}$ is distributed as a multivariate Gaussian $\mathcal{N}(0, \mathbf{G}_{\text{n}})$ with mean zero and covariance matrix $\mathbf{G}_{\text{n}}$.

In practice, the data available are daily cumulative counts of diagnosed individuals j_m, diagnosed recovered r_m and diagnosed dead d_m, $m = 1, ..., M$, see [6]. Putting the three blocks of data together we have

$$\mathbf{d} = (\tilde{j}_1, ..., \tilde{j}_M, r_1, ..., r_M, d_1, ..., d_M), \tag{18}$$

where $\tilde{j}_m = j_m - r_m - d_m$ are the active diagnosed, those who are neither dead nor recovered. Following [31], we define the observation operator as

$$\mathbf{f}(\boldsymbol{\nu}) = (J(1), ..., J(M), R_J(1), ..., R_J(M), D_J(1), ..., D_J(M)), \tag{19}$$

where the dynamics of the diagnosed recovered R_J and diagnosed dead D_J are governed by (10) whereas the diagnosed individuals J in which the infection is active are governed by (4) for SIJR (see Appendix 8 for analytic expressions) or (1) for SEIJR. In (16), we compare these observations to the data $\boldsymbol{d}$ using the distance $\frac{1}{2}\|\mathbf{f}(\boldsymbol{\nu}) - \mathbf{d}\|^2_{\mathbf{G}_n^{-1}}$. To simplify, we consider the noise level for all observations to be uncorrelated, so that $\mathbf{G}_n$ is a real diagonal matrix, $\mathbf{G}_n = \mathrm{diag}(\sigma_1^2, \ldots, \sigma_L^2)$, and set all the variances for the same magnitude equal to a constant $\sigma_J^2, \sigma_R^2, \sigma_D^2$. Thus, $\sqrt{|\mathbf{G}_n|} = \sigma_J^M \sigma_R^M \sigma_R^M$, where $L = 3M$ is the number of data considered. Note that these cost functionals require more information than those based on total case counts: we distinguish diagnosed individuals who are dead, recovered and still sick, and compare with model predictions for them discarding the contribution of the undiagnosed, unlike [11, 13].

4.3   Posterior distribution

Combining (15) with (16) and neglecting normalization constants, the posterior density becomes, up to multiplicative constants,

$$p_{\mathrm{pt}}(\boldsymbol{\nu}) \sim \exp\left(-\frac{1}{2}\|\mathbf{f}(\boldsymbol{\nu}) - \mathbf{d}\|^2_{\mathbf{G}_n^{-1}} - \frac{1}{2}\|\boldsymbol{\nu} - \boldsymbol{\nu}_0\|^2_{\mathbf{G}_{\mathrm{pr}}^{-1}}\right). \tag{20}$$

By sampling this posterior distribution, we can visualize the uncertainty in the inference of parameters for a given data set. To do so, we will resort to Markov Chain Monte Carlo Sampling [8, 27]. Once we have a large collection of samples, we can extract information from the model (2)-(7) with quantified uncertainty, such as the global number of people who have been affected by the virus the last day of the period we are considering. In the next sections we exemplify the procedure for the different stages of the epidemic as observed in Figure 1.

5   Uncertainty in the initial stage

The initial stage of the epidemic corresponds to spread in the absence of any contention measures, see data reproduced in Fig. 3(a)-(b). Our goal here is to first fit the coefficients of the models to such data with quantified uncertainty and then estimate a range of values for the total number of affected individuals at the end of the period, including exposed and undiagnosed infected individuals.

We use the guess obtained in Section 3 as a mean for the prior distribution (15), that is,

$$\boldsymbol{\nu}_0 = (t_{\mathrm{in},0}, \beta_0, \gamma_{2,0}, \delta_0, \alpha_0, \ell_0), \quad \gamma_{1,0}^{-1} = \gamma_{2,0}^{-1} + \alpha_{1,0}^{-1}. \tag{21}$$

For the different rate parameters, the deviations σ_i will not be large. In the absence of a better insight we can take $\sigma_i = 0.1$, $i = 2, .., n$, for instance. The first day of the outbreak is subject to the largest variance. We usually set $\sigma_1 = 10$. For the likelihood (16), we set $M = 20$ (first 20 days) with deviations $\sigma_J = \sigma_R = 10^3$ and $\sigma_D = 10^2$. We then sample the posterior distribution (20) by MCMC techniques [27]. Sampling is initialized with W walkers drawn from the prior distribution, which generate W chains mixed during K steps depending on an acceptance parameter a. Discarding the first B samples produced (to account for the so-called burn in period), we use the remaining $S = KW - B$ samples to draw histograms representing the marginal probabilities of the different
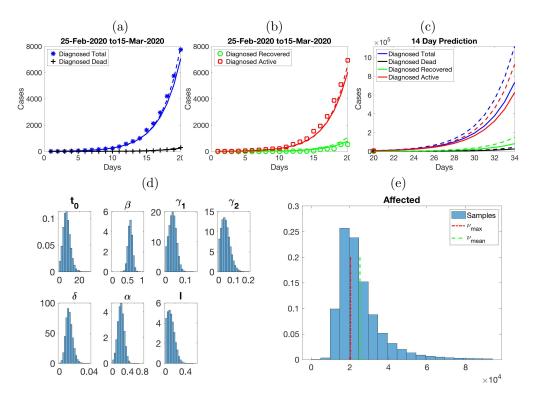
9

Figure 3: Initial stage (free spread): (a) counts of diagnosed and dead cases compared to SIJR solutions of (4) and (10) for $\boldsymbol{\nu}_{\max}$ (solid) and $\boldsymbol{\nu}_{\mathrm{mean}}$ (dashed), (b) same for counts of recovered and active cases, (c) SIJR simulations of the dynamics of diagnosed recovered, dead, active and total cases for $\boldsymbol{\nu}_{\max}$ (solid) and $\boldsymbol{\nu}_{\mathrm{mean}}$ (dashed). Histograms representing (d) a discrete approximation to the probability distribution of parameters and (e) probabilities for the total number of people affected by the virus at the end of the period. The affected people are 25327 for $\boldsymbol{\nu}_{\mathrm{mean}}$ and 20465 for $\boldsymbol{\nu}_{\max}$. Sampling parameters $W = 500$, $S = 4 \times 10^6$, $B = S/4$, and acceptance parameter $a = 2$.

model parameters, see Figure 3 (d). We set $\boldsymbol{\nu}_{\max}$ to be the sample with largest posterior probability and $\boldsymbol{\nu}_{\mathrm{mean}}$ the mean of the parameter samples, see Table 2.

Derived magnitudes can be visualized through histograms too, such as the final number of affected people in Figure 3 (e). It has been calculated solving equations (2)-(8) with the samples as coefficients and computing $A = I + J + R + D$ at the final time, 20 days. We have superimposed the predictions for $\boldsymbol{\nu}_{\max}$ and $\boldsymbol{\nu}_{\mathrm{mean}}$. Note that $\boldsymbol{\nu}_{\max}$ does not have a statistical meaning, it keeps track of a possible best fit to the data. On the other hand, $\boldsymbol{\nu}_{\mathrm{mean}}$ represents some kind of average behavior. When the distributions under study are symmetric, it will be close to $\boldsymbol{\nu}_{\max}$. Otherwise, it may depart from it. In our case, slight asymmetry is caused by discarding negative values. In principle, we could try to improve our estimate of the parameter values that maximize the likelihood by optimization procedures [8]. In practice, enforcing the positivity constraint while doing it may be problematic, and the best samples provide reasonable approximations for our purposes.
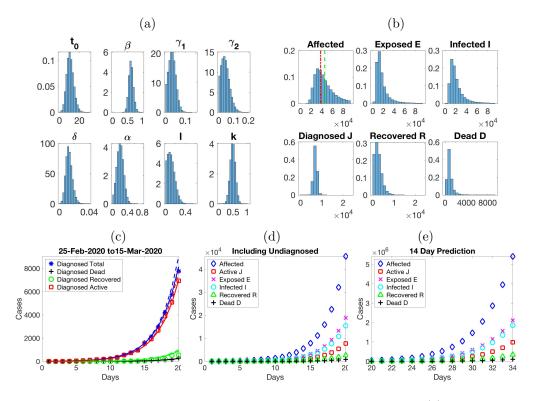
Figure 4: Initial stage using the SEIJR model: Histograms representing (a) a discrete approximation to the probability distribution of some parameters and (b) the probability of different populations at the end of the period, including the total number of people affected by the virus at that time. The affected people are 45515 for $\boldsymbol{\nu}_{\text{mean}}$ (green dashed line) and 37812 for $\boldsymbol{\nu}_{\text{max}}$ (red dot-dashed line). Data for diagnosed, dead, recovered and active cases are compared to solutions of (1) and (10) for $\boldsymbol{\nu}_{\text{max}}$ (solid) and $\boldsymbol{\nu}_{\text{mean}}$ (dashed) in (c). SEIJR predictions of the numbers of exposed, infective, recovered and dead for $\boldsymbol{\nu}_{\text{mean}}$, including undiagnosed and asymptomatic individuals, are shown in (d) for the initial period and in (e) for a later time. Sampling parameters $W = 500$, $S = 4 \times 10^6$, $B = S/4$, and $a = 2$.

Panels (a)-(b) in Fig. 3 compare the observations that would be obtained with $\boldsymbol{\nu}_{\text{max}}$ and $\boldsymbol{\nu}_{\text{mean}}$ to the original data. If we solve the SIJR model for a longer time, for instance, 14 days more, we reach about $8 - 10 \times 10^5$ diagnosed individuals, see panel (c), and about $2.25 - 3.57 \times 10^6$ affected people in the absence of contention measures.

The number of people affected by the virus with a SIJR model $I + J + R + D$ does not consider exposed individuals E. If we wish to estimate them, we need to use the SEIJR model. Figure 4 summarizes some results, quite similar to those for SIJR except for the magnifying effect of including the exposed E. The number of affected individuals $E + I + J + R + D$ increases considerably, however the variation in $I + J + R + D$ is small: 22375 for $\boldsymbol{\nu}_{\text{max}}$ and 26687 for $\boldsymbol{\nu}_{\text{mean}}$ instead of 20465 and 25327 for SIJR, respectively. See Table 2 for a comparison of the parameter values for both models. Note the high transmission rate β (about 0.6) and the low diagnosis rate

α (about 0.2). Most infected individuals are not detected. If we solve the SEIJR model for a longer time, for instance, 14 days more, we reach about $8 - 10 \times 10^5$ diagnosed individuals and $3.6 - 5.4 \times 10^6$ affected people for $\boldsymbol{\nu}_{\mathrm{max}}$ and $\boldsymbol{\nu}_{\mathrm{mean}}$ in the absence of contention measures.

	$\boldsymbol{\nu}_{\mathrm{mean}}$ SIJR	$\boldsymbol{\nu}_{\mathrm{mean}}$ SEIJR	$\boldsymbol{\nu}_{\mathrm{max}}$ SIJR	$\boldsymbol{\nu}_{\mathrm{max}}$ SEIJR	$\boldsymbol{\nu}_0$
t_{in}	7.3786	10.7869	8.3266	11.3098	12.3388
β	0.5938	0.6223	0.5890	0.6078	0.6262
γ_1	0.0390	0.0370	0.0321	0.0349	0.0667
γ_2	0.0473	0.0452	0.0372	0.0417	0.1000
δ	0.0135	0.0129	0.0115	0.0117	0.1000
α	0.2230	0.2051	0.2366	0.2161	0.2000
ℓ	0.1104	0.1138	0.0625	0.0694	0.0714
q		0.4947		0.4975	0.5000
k		0.4966		0.4809	0.5000
$\log(p_{\mathrm{post}})$	-2.1343		-1.1836		-119.2493
$\log(p_{\mathrm{post}})$		-1.9204		-1.0640	-58.1152

Table 2: Values of $\boldsymbol{\nu}_{\mathrm{mean}}$ and $\boldsymbol{\nu}_{\mathrm{max}}$ during the initial stage using the SIJR and SEIJR models.

In the next section we study the influence of contention measures on the subpopulations by means of the SEIJR model distinguishing two populations, one of which is confined.

6   Incorporating the effect of contention measures

To incorporate the effect of confinement we consider the SEIJR model with two populations S_1 (unconfined) and S_2 (confined). During the first period of free growth $[t_{\mathrm{in}}, T_1]$, we have $S_2 = 0$. The different periods for the data shown in Fig 1(a) are marked by variations in these populations as a result of confinement measures. In each $i-$th period $[T_{i-1}, T_i]$, $i > 1$, we solve the SEIJR model (1) using as initial values the final values from the previous period at T_{i-1}, for all the variables except for S_1 and S_2:

- Period 2: $(1 - \rho)S_1(T_1)$ and $S_2(T_1) + \rho S_1(T_1)$ are used as initial data for S_1 and S_2, respectively.

- Period 3: $(1 - \rho)S_1(T_2)$ and $S_2(T_2) + \rho S_1(T_2)$ are used as initial data for S_1 and S_2, respectively.

- Period 4: $S_1(T_3) + (1 - \rho)S_2(T_3)$ and $\rho S_2(T_3)$ are used as initial data for S_1 and S_2, respectively.

Recall that in the first period, the initial values for all the variables are zero, except $E(t_{\mathrm{in}}) = 1$ and $S_1(t_{\mathrm{in}}) = N - 1$. No parameter t_{in} appears in the next periods, we set it equal to zero. Instead, we introduce $\rho \in (0, 1)$ to quantify the abrupt changes in the fraction of people confined at the start of each period. We assume that the transmission rate for S_2 is lower by a factor p, that is, $p\beta$ instead of β, due to the reduction of contacts with other people. Due to possible interaction with already sick people or people still working outside at home, we cannot set it equal to zero.

We adapt the framework presented in Section 4 ensambling these periods as we explain next. To consider stages i, $i = 1, \ldots, Q$, we multiply the number of parameters by Q. The first block
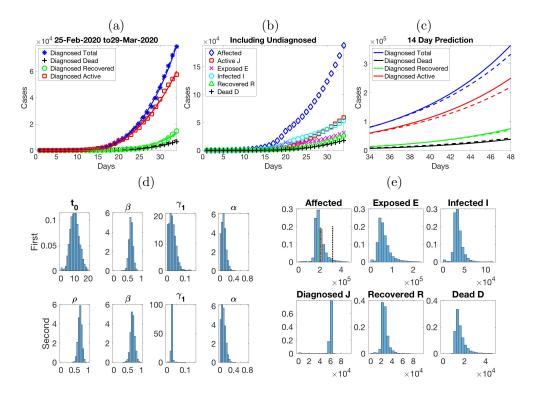
Figure 5: First and second periods: (a) Data for diagnosed (asterisks), dead (crosses), recovered (triangles) and active (squares) cases, compared to solutions of (1) and (10) for $\boldsymbol{\nu}_{\max}$ (solid) and $\boldsymbol{\nu}_{\mathrm{mean}}$ (dashed), extended in (c) for a longer time. (b) SEIJR simulations of the numbers of exposed, infective, recovered and dead individuals for $\boldsymbol{\nu}_{\mathrm{mean}}$ including the undiagnosed and asymptomatic. (d) Histograms comparing the distribution of some parameters in the two periods. (e) Histograms representing the probability of the status of different populations at the end. Vertical lines mark the values for $\boldsymbol{\nu}_{\max}$ (red dot-dashed line), $\boldsymbol{\nu}_{\mathrm{mean}}$ (green dashed line), and the mean for all samples (black dotted line). Sampling parameters $W = 500$, $S = 4 \times 10^6$, $B = S/4$ and $a = 2$.

of 9 parameters is the standard one for the first period. The remaining blocks correspond each to one additional period, with t_{in} replaced by ρ. We keep the same initial guesses of the parameters used in Section 5 as prior knowledge in all the periods, except for ρ, which is set equal to $3/4$, $4/5$, $15/16$ respectively, an approximation of the population switches at the different stages. The deviations are kept equal to 0.1 for all, except t_{in}, for which we set it equal to 10. As for the data, we keep the same deviations as in Section 5 in all the periods, in the absence of better information.

Let us consider first the initial confinement period. Figure 5(a) compares to data the evolution of the diagnosed subpopulations. Population dynamics is calculated solving the SEIJR model in two sequential steps, in $[t_{\mathrm{in}}, T_1]$ and $[T_1, T_2]$, using in each of them the parameter values obtained for that period and the initial data stipulated earlier. Panel (b) represents the solutions of the SEIRJ model including the contribution of undiagnosed and asymptomatic individuals. Panel (d) compares the distribution of some parameters in the two periods. The transmission rate β

increases slighty in the second period, while the diagnose rate remains low. These histograms are discretizations of the probability, so that the height of each bin is the number of samples divided by the total and by the basis of the bins (which is the same for the histograms corresponding to the same parameters in this figure and the previous ones to allow for comparisons). Figure 5(e) quantifies uncertainty in the total number of people affected by the virus after these two periods. If we keep the parameter values $\boldsymbol{\nu}_{\max}$ or $\boldsymbol{\nu}_{\mathrm{mean}}$ up to time $T_3 > T_2$, growth slows down, but it does not stabilize, see Fig. 5(c).

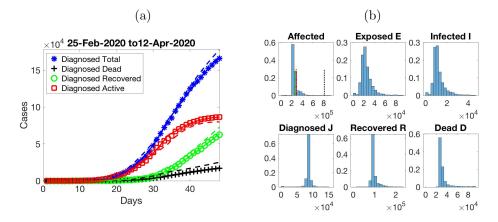(a)   (b)

Figure 6: Same as Fig. 5(a) and (e) for three periods of increasing confinement. Note the decrease in the numbers of exposed E and infected I cases. Sampling parameters $W = 500$, $S = 5 \times 10^6$, $B = S/4$ and $a = 2$.

We incorporate next the third additional period in which an even larger fraction of the population is confined at home. The results are reproduced in Figure 6. Finally, the growth trend moderates, also in predictions for longer times, see Fig 2(b). Table 3 reports the mean values $\boldsymbol{\nu}_{\mathrm{mean}}$ obtained after MCMC sampling, as well as the values corresponding to the best sample $\boldsymbol{\nu}_{\max}$. As mentioned earlier, $\boldsymbol{\nu}_{\max}$ has not a statistical meaning. It represents a best fit whose coefficients may fluctuate a bit with the number of samples. Instead, $\boldsymbol{\nu}_{\mathrm{mean}}$ conveys a statistical trend of the coefficients of the samples. Comparing the values of β for $\boldsymbol{\nu}_{\mathrm{mean}}$, we remark an increase in β in the second period. This fact is also observed in $\boldsymbol{\nu}_{\max}$ and the trend was already present in the histograms for β in Fig 5(d). According to the information available on the spanish outbreak, and taking into account that infected people can take up to 14 days to show symptoms, this might be a delayed reflection of crowd gatherings occurred at the end of the first period, or also, a result of the lack of protective equipment for overwhelmed health care and security workers. We also observe a reduction in the mean recovery rates for γ_1 and γ_2 in the second period, which may be reflection of the saturation of the health care system and the scarceness of medical resources during the second period. Notice that the diagnose rate α is quite low. A large fraction of affected people remains undetected.

In a fourth period, a fraction of the population is released from confinement. The number of undiagnosed and exposed individuals is depleted and the spread of the epidemic is contained. Unlike before, the SEIJR solutions for $\boldsymbol{\nu}_{\max}$ still fit the data quite well, but the solutions for $\boldsymbol{\nu}_{\mathrm{mean}}$ deviate from the data towards the solution for the prior $\boldsymbol{\nu}_0$, see Fig. 7(a). This reflects some kind

14

	ν_{mean} 1st	ν_{mean} 2nd	ν_{mean} 3rd	$\nu_{\max}$ 1st	ν_{mean} 2nd	$\nu_{\max}$ 3rd
$t_{\mathrm{in}},\ \rho$	12.3479	0.7202	0.2236	7.9770	0.8064	0.2527
β	0.6173	0.6902	0.5898	0.6894	0.7028	0.6796
γ_1	0.0741	0.0363	0.0446	0.0410	0.0290	0.0318
γ_2	0.1426	0.0437	0.0551	0.0532	0.0343	0.0461
δ	0.0696	0.0310	0.0131	0.0141	0.0180	0.0098
α	0.1541	0.2148	0.2343	0.1791	0.1851	0.1022
ℓ	0.1056	0.1245	0.1031	0.1253	0.1800	0.0219
q	0.4978	0.5301	0.5082	0.3872	0.7778	0.4234
p		0.1139	0.0643		0.1845	0.0001
k	0.4984	0.5106	0.5251	0.5802	0.5703	0.5339

Table 3: Values of $\boldsymbol{\nu}_{\mathrm{mean}}$ and $\boldsymbol{\nu}_{\max}$ for three periods using the SEIJR model, with $\log(\boldsymbol{\nu}_{\mathrm{mean}}) = 3.2974$, $\log(\boldsymbol{\nu}_{\max}) = 188$, $\log(\boldsymbol{\nu}_0) = -71097$, respectively. In the first row, the first columns represent t_0, while the rest correspond to ρ.
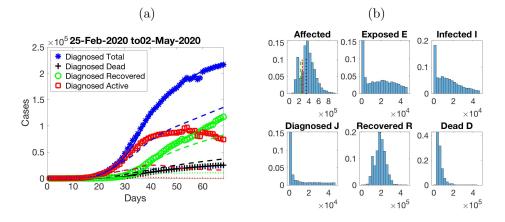

Figure 7: Same as Fig. 6(a)-(b) for four periods. Additional dotted lines in the lower part of panel (a) represent solutions of (1) and (10) for $\boldsymbol{\nu}_0$. The numbers of exposed E, infected I and active diagnosed J individuals are depleted.

of bimodality, with a collection of SEIJR solutions close to the prior while most of them remain close to the data as the model coefficients range through the sampled parameters. This may be a consequence of fixing prior guesses for the model parameters that worsen with time. Note that the predictions that would be obtained using the prior are rather poor, compared to true counts, as time grows. However, the predictions provided by $\boldsymbol{\nu}_{\max}$ fit the data quite well, even for later times, see Fig. 2(b).

Note that as we add data from new periods, we are including more information in the analysis. The best coefficient values estimated for previous periods change slightly and we infer more moderate numbers of affected individuals, as compared with the previous studies done using less data. However, the same trends persist: increase of β in the second period, while γ_1 and γ_2 decrease, decrease of δ and low diagnose rate α. Very few tests were done during these periods. In fact, the usefulness of tests would be to increase the diagnose rate, augmenting the number of quarantined

infected and asymptomatic individuals.

Figure 2(b) provides a global view of our analysis. Shaded areas represent the total number of diagnosed cases $J + D_J + R_J$ obtained solving (1) and (10) for the last 1000 sampled parameters in each of the four frameworks we have considered: red for Period 1, green for Periods 1-2, blue for Periods 1-2-3, magenta for Periods 1-2-3-4. Dotted lines represent the mean of the curves obtained for all the samples. Thicker lines represent the total number of diagnosed cases $J + D_J + R_J$ for $\boldsymbol{\nu}_{\max}$ (solid), $\boldsymbol{\nu}_{\mathrm{mean}}$ (dashed) and $\boldsymbol{\nu}_0$ (dash-dotted). Yellow circles represent the data: total counts of diagnosed people (dead, recovered and active). Colored triangles separate the 'inference' from the 'prediction' regions for each of them. At the back of the triangles, we have the inference region, corresponding to the data we use to infer the parameter values and the total number of affected people. At the front of the triangles, we use model solutions to predict the time evolution keeping the conditions of the last period considered in the inference studies. Taking no measures leads to the evolution represented in red. Confining people who are able to work online or do not work in basic activities results in the dynamics marked in green. Extending the confinement to all the population not working in strictly essential activities leads to the forecast painted in blue. Releasing this last fraction of the population results in the evolution represented in magenta. Notice that the solid magenta curve corresponding to $\boldsymbol{\nu}_{\max}$ agrees very well with the data past day 68 (last day used to calculate it), whereas some magenta samples deviate considerably. This fact is reflected in the dotted averages, which define somehow a confidence region. After day 68 the population was released from confinement by stages, and the use of masks was enforced, lowering the risk for the users. The country remained closed. The different predictions associated to the four inference studies we carried out are not only due to the confinement or the release of population fractions, but to the fact that we allow for variations in the model coefficients in the different periods to adapt them to additional amounts of data. The fact that the transmission coefficient β decreases with time due to improved conditions is fundamental.

These studies are limited by the data quality. As mentioned earlier, the order of magnitude of the population counts in official records changes noticeably when only PCR confirmed cases are taken into account or also probable cases are included. In the spanish outbreak, the number of probable cases may have been five times higher and the number of dead individuals twice as much. Repeating our previous studies scaling the data in that way, we find estimates about 2 million people, consistent with the official conclusions inferred from selected testing campaings.

7 Conclusions

The attempt to devise mathematical models to study the progression of a pandemic faces the need to handle large uncertainty in the available data. We have developed a Bayesian framework to quantify uncertainty in the effects of lockdown measures through the coefficients of SEIJR and SIJR models for human-to-human transmission. A key idea is the introduction of two populations, one of which has a lower risk of infection than the other. Lower risk may be due to confinement, as it happens for the data we consider here, or to preventive measures, such as the use of masks. Therefore, our methodology is not constrained to lockdown measures.

These techniques allow us to calibrate important magnitudes to forecast the evolution of the epidemic, such as the variation in the total number of affected people (including asymptomatic individuals), and could be adapted to infer coefficients from data from any country. We show how enforcing measures that deplete the number of undiagnosed and asymptomatic individuals, while

16

reducing the transmission rate, we can stop the spread. We have focused on the data available for Spain, which shows well differentiated data periods according to the measures taken. We see that the model coefficients in each period vary with the circumstances. For instance, transmission rates may augment as a result of increased interaction and lack of protective measures and recovery rates may decrease as a result of scarceness of resources. The diagnose rate is low, resulting in large number of undiagnosed individuals. Performing more PCR tests increases the diagnose rate, allowing to quarantine more infected and asymptomatic individuals.

An additional difficulty when applying this inference framework for large periods of time (months) is the fact that uncertainty in the observed data accumulates over time when using cumulative data. This poses the problem of selecting adequate variances for the analysis. In the absence of reliable information in that respect, we have kept them fixed. Calculations with daily data do not show significative differences in the observed trends in our case. Moreover, we have used official data for PCR confirmed patients only. The effect of adding probable cases, which may have been five times higher, would require further consideration.

SIR type models assume that recovered individuals have immunity. This may not be the case here, thus additional studies taking this factor into account would be advisable [23, 30]. Furthermore, standard SIR type models [28] are formulated for closed systems. Introducing spatial mobility [4, 28] is an important issue that should be a subject for future work. Moreover, imperfect implementation of contention measures leads to delays, which might be better described by differential-delay models [33]. We have focused on human-to-human transmission here. Coronaviruses originate in animals, such as bats, and arrive to humans through intermediate animal species which act as reservoirs for future waves [9], subject deserving further studies.

8 Appendix: Solutions of the SIJR model

Let us obtain explicit expressions for the solution of the (2)-(8) model. Consider the equations (3)-(4) for I and J. Set $D_1 = \alpha + \gamma_1 + \delta$, $D_2 = \gamma_2 + \delta$. The system matrix is

$$A = \begin{pmatrix} \beta - D_1 & \ell\beta, \\ \alpha & -D_2, \end{pmatrix}$$

with eigenvalues

$$\lambda_1 = \frac{\beta - D_1 - D_2}{2} - \frac{1}{2}\sqrt{\beta^2 - 2\beta D_1 + 2\beta D_2 + 4\alpha\ell\beta + D_1^2 - 2D_1 D_2 + D_2^2},$$

$$\lambda_2 = \frac{\beta - D_1 - D_2}{2} + \frac{1}{2}\sqrt{\beta^2 - 2\beta D_1 + 2\beta D_2 + 4\alpha\ell\beta + D_1^2 - 2D_1 D_2 + D_2^2},$$

and eigenvectors:

$$\mathbf{v}_1 = (-\ell\beta, \, \beta - D_1 - \lambda_1), \quad \mathbf{v}_2 = (-\ell\beta, \, \beta - D_1 - \lambda_2).$$

The general solution is

$$(I(t), J(t)) = z_1\mathbf{v}_1 e^{\lambda_1 t} + z_2\mathbf{v}_2 e^{\lambda_2 t}, \quad z_1, z_1 \in \mathbb{R}.$$

We obtain the solutions for the initial value problem combining the solutions with initial data $(1, 0)$ and $(0, 1)$. The coefficients z_1, z_2 for $(0, 1)$ are

$$z_1 = -1/(\lambda_1 - \lambda_2), \quad z_2 = 1/(\lambda_1 - \lambda_2).$$

For $(1, 0)$

$$z_1 = (D_1 - \beta + \lambda_2)/(\beta \ell (\lambda_1 - \lambda_2)), \quad z_2 = -(D_1 - \beta + \lambda_1)/(\beta \ell (\lambda_1 - \lambda_2)),$$

provide the solution to our problem.

Set

$$c_1 = \frac{\beta - D_1 - \lambda_2}{\lambda_1 - \lambda_2}, c_2 = \frac{\beta - D_1 - \lambda_1}{\lambda_2 - \lambda_1}.$$

Then the number of infected people is

$$I(t) = c_1 e^{\lambda_1 t} + c_2 e^{\lambda_2 t}, \tag{22}$$

and the cumulative number of infected people I_c such that $I_c' = I$, $I_c(0) = 0$, is

$$I_c(\beta, t) = \frac{c_1}{\lambda_1} e^{\lambda_1 t} + \frac{c_2}{\lambda_2} e^{\lambda_2 t} - \left(\frac{c_1}{\lambda_1} + \frac{c_2}{\lambda_2} \right). \tag{23}$$

The number of diagnosed people is

$$J(t) = \frac{\alpha}{\lambda_1 - \lambda_2} e^{\lambda_1 t} + \frac{\alpha}{\lambda_2 - \lambda_1} e^{\lambda_2 t}. \tag{24}$$

The cumulative number of diagnosed people J_c is then the integral of this magnitude, $J_c' = J$ starting from zero $J(0) = 0$:

$$J_c(t) = \frac{\alpha}{\lambda_1 - \lambda_2} \left(\frac{e^{\lambda_1 t} - 1}{\lambda_1} - \frac{e^{\lambda_2 t} - 1}{\lambda_2} \right). \tag{25}$$

We can now integrate the equations for S, R and D:

$$S(t) = -\beta I_c(t) - \beta \ell J_c(t), \tag{26}$$
$$R(t) = \gamma_1 I_c(t) + \gamma_2 J_c(t), \tag{27}$$
$$D(t) = \delta I_c(t) + \delta J_c(t). \tag{28}$$

If we work with the diagnosed recovered and the diagnosed dead, we get

$$R_J(t) = \gamma_2 J_c(t), \tag{29}$$
$$D_J(t) = \delta J_c(t). \tag{30}$$

The formulas given here set $t_{\mathrm{in}} = 0$. To use them with initial data at a generic t_{in} we just replace t by $t + t_{\mathrm{in}}$ in the formulas obtained here.

18

References

[1] Ambikapathy B, Krishnamurthy K. Mathematical modelling to assess the impact of lockdown on covid-19 transmission in India: Model development and validation. JMIR Public Health Surveillance 2020;6(2) DOI:10.2196/19368.

[2] Al-qaness MAA, Ewees AA, Fan H, Aziz MDE. Optimization method for forecasting confirmed cases of covid-19 in China. Journal of Clinical Medicine 2020;9(674).

[3] Anderson RM, May RM. Population biology of infectious diseases: Part I. Nature Publishing Group. 1979;280(5721):361-367.

[4] Bouchnita A, Jebran A. A hybrid multi-scale model of covid-19 transmission dynamics to assess the potential of non-pharmaceutical interventions. Chaos, Solitons & Fractals 2020;138:109941.

[5] Brauner JM, Mindermann S, Sharma M, Stephenson AB, Gavenciak T, Johnston D, Salvatier J, Leech G, Besiroglu T, Altman G, Ge H, Mikulik V, Hartwick M, Teh YW, Chindelevitch L, Gal Y, Kulveit J. The effectiveness and perceived burden of nonpharmaceutical interventions against covid-19 transmission: A modelling study with 41 countries. medRxiv (2020). DOI 10.1101/2020.05.28.20116129

[6] Enfermedad por el coronavirus (covid-19), Actualizaciones n° 30 - n° 135, Centro de Coordinación de Alertas y Emergencias Sanitarias, Ministerio de Sanidad, Gobierno de España, 2020.

[7] Capistran MA, Christen JA, Velasco-Hernandez JX. Towards uncertainty quantification and inference in the stochastic SIR epidemic model. Mathematical biosciences. 2011:24(2):250-259.

[8] Carpio A, Iakunin S, Stadler G. Bayesian approach to inverse scattering with topological priors. Inverse Problems 36, 105001 (2020).

[9] Chen TM, Rui J, Wang QP, Zhao ZY, Cui JA, Yin L. A mathematical model for simulating the phase-based transmissibility of a novel coronavirus. Infectious Diseases of Poverty 2020;9:24

[10] Chowell G, Fenimore PW, Castillo-Garsow MA, Castillo-Chavez C, SARS outbreak in Ontario, Hong Kong and Singapore: the role of diagnosis and isolation as a control mechanism, Los Alamos Unclassified Report LA-UR-03-2653, 2003.

[11] Dehning J, Zierenberg J, Spitzner FP, Wibral M, Neto JP, Wilczek M, Priesemann V. Inferring change points in the spread of covid-19 reveals the effectiveness of interventions. Science (2020). DOI 10.1126/science.abb9789

[12] Diekmann O, Heesterbeek JAP. Mathematical Epidemiology of Infectious Diseases: Model Building, Analysis and Interpretation. John Wiley and Sons; 2000.

[13] Ding G, Chang L, Gong J, Wang L, Cheng K, Zhang D. SARS epidemical forecast research in mathematical model. Chinese Science Bulletin 2004;49:2332-2338

[14] Engbert R, Rabe MM, Kliegl R, Reich S. Sequential data assimilation of the stochastic SEIR epidemic model for regional covid-19 dynamics. medRxiv (2020). DOI 10.1101/2020.04.13.20063768

[15] Ferguson NM, Laydon D, Nedjati-Gilani G. et al, Impact of non-pharmaceutical interventionsv (NPIs) to reduce covid-19 mortality and healthcare demand. Imperial College Lond (16-03-2020) (2020). DOI 10.25561/77482

[16] Ferrari L, Gerardi G, Manzi G, Micheletti A, Nicolussi F, Salini S, Modelling provincial covid-19 epidemic data in Italy using an adjusted time-dependent SIRD model, arXiv preprint arXiv:2005.12170

[17] Flaxman S, Mishra S, Gandy A, Unwin HJT , Mellan TA, Coupland H, Whittaker C, Zhu H, Berah T, Eaton JW, Monod M, Imperial College covid-19 Response Team, Ghani AC, Donnelly CA, Riley SM, Vollmer MAC, Ferguson NM, Okell LC, Bhatt S. Estimating the effects of non-pharmaceutical interventions on covid-19 in Europe. Nature (2020). DOI 10.1038/s41586-020-2405-7

[18] Huppert A, Katriel G. Mathematical modelling and prediction in infectious disease epidemiology. Clinical Microbiology and Infection. 2013;19(11):999-1005.

[19] Análisis de los casos de covid-19 notificados a la RENAVE hasta el 10 de mayo en España, Informe covid-19 n° 33, Instituto de Salud Carlos III, 29 de mayo de 2020

[20] Kaipio J, Somersalo E, Statistical and computational inverse problems 160. Springer Science & Business Media; 2006.

[21] Kermack WO, McKendrick AG. A contribution to the mathematical theory of epidemics. Proceedings of the Royal Society of London Series A. 1927;115(772):700-721.

[22] Khailaie S, Mitra T, Bandyopadhyay A, Schips M, Mascheroni P, Vanella P, Lange B, Binder S, Meyer-Hermann M. Estimate of the development of the epidemic reproduction number Rt from coronavirus SARS-CoV-2 case data and implications for political measures based on prognostics. medRxiv (2020). DOI 10.1101/2020.04.04.20053637

[23] Kissler SM, Tedijanto C, Goldstein E, Grad YH, Lipsitch M. Projecting the transmission dynamics of SARS-CoV-2 through the postpandemic period. Science 2020;368(6493):860-868.

[24] Kucharski AJ, Russell TW, Diamond C, Liu Y, Edmunds J, Funk S, Eggo RM. Early dynamics of transmission and control of covid-19: a mathematical modelling study. The Lancet (2020), DOI 10.1016/S1473-3099(20)30144-4

[25] Kuniya J. Prediction of the epidemic peak of coronavirus disease in Japan. Journal of Clinical Medicine. 2020;9(789). DOI 10.3390/jcm9030789.

[26] R. Fletcher, Modified Marquardt subroutine for non-linear least squares, Tech. Rep. 197213, 1971.

[27] Foreman-Mackey D, Hogg DW, Lang D, Goodman J. emcee: The MCMC Hammer. Publications of the Astronomical Society of the Pacific 2013;125(925).

[28] Li R, Pei S, Chen B, Song Y, Zhang T, Yang W, Shaman J. Substantial undocumented infection facilitates the rapid dissemination of novel coronavirus (SARS-CoV2). Science (2020) DOI 10.1126/science.abb3221

[29] Nishiura H, Linton NM, Akhmetzhanov AR. Serial interval of novel coronavirus (covid-19) infections. International Journal of Infectious Disease. 2020;93:284-286.

[30] Ng KY, Gui MM. covid-19: Development of a robust mathematical model and simulation package with consideration for ageing population and time delay for control action and resusceptibility. Physica D: Nonlinear Phenomena 2020;411-132599.

[31] Pierret E, Uncertainty quantification in SARS epidemics. Report for the 'Jacques Hadamard' Master's Research Internship. ENS Paris Saclay - UCM; 2020.

[32] Rothana HA, Byrareddy SN, The epidemiology and pathogenesis of coronavirus disease (covid-19) outbreak. Journal of Autoimmunity 2020;109:102433.

[33] Ruschel S, Pereira T, Yanchuk S, Young LS, An SIQ delay differential equations model for disease control via isolation. Journal of Mathematical Biology 2019;79:249-279.

[34] Sesterhenn JL. Adjoint-based data assimilation of an epidemiology model for the covid-19 pandemic in 2020. arXiv preprint arXiv:2003.13071

[35] Tiwari S, Kumar S, Guleria K. Outbreak trends of coronavirus (covid-19) in India: A prediction. Disaster Medicine and Public Health Preparedness. 2020 DOI 10.1017/dmp.2020.115.

[36] Zhu N, Zhang D, Wang W, Li X, Yang B, Song J, Zhao X, Huang B, Shi W, Lu R, Niu P, Zhan F, Ma X, Wang D, Xu W, Wu G, Gao GF, Tan W. A novel coronavirus from patients with pneumonia in China. N. Engl. J. Med. 2020:382(8), 727-733.